



Investigation of Morphological, Elemental, Structural, and Optical Properties of Fe-Doped TiO₂ Nanoparticles

Muhammad Irfan Ahmad¹, Hafiz Muhammad Asif Javed^{1*}, Asad Ali¹, Zaheer Ul Hassan¹, M. Afzaal², Muhammad Arif³, Shahid Hussain⁴

¹ Nanomaterials and Solar Energy Research Laboratory, Department of Physics, University of Agriculture Faisalabad, 38000, Faisalabad, Pakistan

² Department of Physics, Riphah International University Faisalabad Campus, Pakistan

³ NFC Institute of Engineering and Fertilizer Research, Faisalabad, Pakistan

⁴ School of Materials Science and Engineering, Jiangsu University, 212013, Zhenjiang, China

ARTICLE INFO

ABSTRACT

Article History:

Received: March 24, 2022
Revised: May 29, 2022
Accepted: June 29, 2022
Available Online: June 30, 2022

Keywords:

TiO₂ Nanoparticles
Fe-Doped TiO₂ Nanoparticles
Morphological Analysis
Elemental Analysis
Structural Analysis
UV/Vis Spectra Analysis

In this research, Fe-doped TiO₂ nanoparticles were synthesized by sol-gel technique followed by annealing at 450 °C in a vacuum. The effects of Fe-doping on the morphological, elemental, structural and optical properties of TiO₂ nanoparticles have been investigated. XRD analysis was performed to examine the structural properties of synthesized pure TiO₂ nanoparticles and Fe-doped TiO₂ nanoparticles. Surface analysis was done using Scanning Electron Microscopy. Optical properties were determined using UV/Vis spectroscopy. Morphological analysis revealed that TiO₂ nanoparticles have a spherical shape. EDX analysis confirmed the elemental composition of Fe-doped TiO₂ nanoparticles. XRD patterns showed that diffraction peaks can be attributed to TiO₂ with the anatase phase.

OPEN ACCESS

© 2022 The Authors, Published by iRASD. This is an Open Access article under the Creative Common Attribution Non-Commercial 4.0

*Corresponding Author's Email: m.asif.javed@uaf.edu.pk

1. Introduction

Nanoparticles are tiny objects that play a vital role in many applications due to their characteristics and functionality. Nanoparticles should have been considered substances with a certain degree of physical state in addition to solid, liquid, and gaseous plasma states due to their unique nature (Larumbe, Monge, & Gómez-Polo, 2015). The synthesis of TiO₂ nanoparticles can be done in various ways, but the Sol-Gel approach is very convenient. It is a more widespread and general approach for synthesising TiO₂ nanoparticles (Yu et al., 2006). When the interactions connecting two particles are sufficiently repulsive, and the surfaces supporting forces prevent agglomeration and coagulation, the solution becomes stable. When another addition removes the charge on the particle, the system collapses (flocculation), resulting in gel formation (Valero-Romero et al., 2019). This procedure involves passing the system through a colloidal form of a liquid sol, which is then transformed into a Sol-Gel phase. Sol is commonly made with an organic metal complex such as a metal alkoxide/inorganic metal salt (Z. Li, Shen, He, & Zu, 2008).

There are two types of Sol-Gel techniques; the first is an aqueous technique that results in an inorganic metal salt. While the other is an alcohol-based process with metal alkoxide as the first precursor. Titanium oxide (TiO₂) is a naturally occurring mineral (Sood, Umar, Mehta, & Kansal, 2015). Titanium oxide is a semiconductor material having band energy equal to or higher than bandgap energy and photocatalytic activity when exposed to sunshine. Titanium dioxide is not found in pure form in the earth but comes from white oxen or limonite ore. Titanium dioxide crystallizes after passing through the amorphous state (Kim, Hong, Kim, Song, & Lee, 2004). Titanium dioxide crystallizes after passing

through the amorphous state. Titanium dioxide is non-poisonous and an incomplete acidic oxide that is synthetically stable. Titanium dioxide is non-poisonous and has a stable synthetic structure. At room temperature, there was no response to various compounds (Nasralla et al., 2013). Titanium dioxide is a fragmentary acidic oxide. The crystalline arrangement of the Titanium nanoparticles largely depends on the preparation procedure. The size of titanium dioxide nanoparticles is lowered, and the number of positioned atoms increases, improving catalytic activity even more. Plastics, coatings, UV-resistant materials, links, and chemical fibers all contain these nanoparticles.

2. Experimental Section

2.1. Synthesis of Fe-Doped TiO₂ Nanoparticles

TiO₂ photocatalysts were prepared using a modified sol-gel technique. Solution A was created by pouring 20 mL of TTIP into 80 mL of 100% ethanol. In addition, 2 mL distilled water and 2 mL H₂SO₄ were blended in 20 mL 100% ethanol to make solution B. Solution B was added dropwise to solution A while vigorously stirred. The gel was created by stirring the solution at room temperature (Ali et al., 2017). The gel was aged at 80°C for 24 hours at room temperature, dried in an oven, and ground to powder. The calcination is carried furnace at 400°C. For an indication of the nanoparticles, the FTO substrates have been first cleaned completely with the help of ethanol and then dried earlier before deposition (Dholam, Patel, Adami, & Miotello, 2009). These substrates were dunked in the viscous pure "TiO₂-sol" of identified consistency after drying at the room-temperature. Following such a strategy, nanoparticles have been kept by antecedent-sol of the various viscosities to contemplating the connection between the consistency of forerunner sol and the thickness of a film. A thin film of Titanium (TiO₂) framed upon the FTO substrate was firstly dried in the air at room-temperature took after drying at the temperature of 80°C for 3 hours in the oven (Einert, Hartmann, Smarsly, & Brezesinski, 2021). The film framed is additionally warmed at the temperature of 400°C for only 1 hour in the furnace in the presence of air. This technique makes the thin film on substrates look like a glass plate. A thin film of titanium dioxide was shaped onto the FTO substrate (Zheng et al., 2022). Also, after warming treatment, these were used for the photocatalytic response. Even though we have arranged films on different types of substrates such as treated steel, aluminium, or clay plates, the films kept on the glass substrates have been contemplated specifically for the auxiliary and photocatalytic conduct for accommodation (Kanjana, Maiaugree, Poolcharuansin, & Laokul, 2021). Hina powder was mixed with ethanol and stirred on the stirrer for one hour without providing heat to obtain the Hina powder solution. For this purpose, the weight of Hina powder was 5gm, and ethanol was 100ml (Kanjana et al., 2021).

FTO was cleaned with ethanol and, using a voltmeter, checked its conducting side. By using tapes, FTO was fixed on the Table. A paste of TiO₂ was deposited on its conducting side, which was dried for 1 hour and dipped into the Hina powder solution for some time, so that layer of dye (Hina Powder) is deposited onto the photo anode for light harvesting (Na et al., 2021). A photoanode of TiO₂ was prepared. We cleaned FTO with ethanol and checked its conducting side using a voltmeter. The FTO was fixed on the Table by using tapes. A paste of the composite of Fe doped TiO₂ was deposited on its conducting side, which was dried for 1 hour (Baruah et al., 2021).

2.2. Characterizations

TiO₂ nanoparticles have been prepared by the method of sol-gel. The precursor used in this method was Titanium tetra-isopropoxide (TTIP). Starting precursor for this method was Titanium tetra-isopropoxide (TTIP). Water and ethanol acted as a solvent in this method, and H₂SO₄ was used as an acidic catalyst, making the reaction much faster than without a catalyst. The prepared titanium dioxide nanoparticles sample was examined using different techniques. The diffraction method characterizes the nanostructure of synthetic Titania nanoparticles. For this purpose, the technique which was used named as Powder XRD method. To determine the structure of crystalline solids, this diffraction method XRD is widely used (Zheng et al., 2022). This method can quickly obtain diffraction data, and this powder method can be applied to all crystalline materials. Each product has unique diffraction data, and powder can be used to easily identify any substance. Samples were characterized by X-ray diffraction (XRD). The crystal size was determined by a formula

known as Scherer's formula. Reduced temperature and crystalline size decrease. SEM observed images of prepared samples, and EDX determined elemental composition and ratio.

3. Results and Discussion

3.1. Morphological Analysis

SEM analysis of the prepared sample of Fe-doped TiO₂ nanoparticles samples. A scanning electron microscope (SEM) is an electron microscope that makes images of a sample by scanning the surface with a focused beam of electrons. And the process of making the sample images is discussed as the electrons interact with atoms in the sample, producing various signals containing information about the surface topography and composition of the sample. The electron beam is scanned in a raster scan pattern. The beam's position is combined with the detected signal to produce an image. SEM can achieve resolution better than 1 nanometer. Samples are observed in high vacuum in conventional SEM, in low vacuum or wet conditions in variable pressure or environmental SEM, and at a wide range of cryogenic or elevated temperatures with specialized instruments. The most common mode of SEM is detecting secondary electrons emitted by atoms when an electron beam strikes them and excites them.

A special detector detects secondary electrons emitted by the electron beam from the sample atoms. The SEM micrographs of the Fe-doped TiO₂ nanoparticles were formed at 400°C for 4h(Sukhadeve et al., 2022). In general, all the Fe-doped TiO₂ nanoparticles show Nano size and have a spherical shape in powder particles. The pure TiO₂ particles range from 1–3µm, and doped particles show about 200 to 500nm in size. A close considers these powders. Micrographs reveal that the degree of assembling initially decreased with the doping of Fe into TiO₂. After that, it gradually increased with the further increase of Fe content in TiO₂ (Xia et al., 2022).

SEM revealed the external morphology, chemical composition, crystalline structure, and orientation of materials making up the sample. The morphology of the Fe-doped TiO₂ nanoparticles is shown in the Figures. It presents clear evidence that uniform-sized particles are spherical in shape. The SEM of the iron-doped TiO₂ samples reveals that the crystals are nanometer-sized. Therefore, the growth of nanophase crystalline TiO₂ particles was accelerated at higher calcined temperatures(Begna, Gurmesa, Zhang, & Geffe, 2022).

All samples show uniform morphology in the form of TiO₂ nanoclusters. It has been observed that the TiO₂ nanoparticles annealed at 400°C almost reveal that the primary particles are quite uniform in size, quite clean, and roughly spherical. The agglomerates are fused to form comparatively smaller irregular grains giving rise to highly porous materials which enhance the photovoltaic performance(Song et al., 2022). The Fe-doped TiO₂ nanoparticles have a larger grain size. It exhibits lesser receptivity and higher transparency, which are important for TCO applications.

Figure 1 shows the SEM images of Fe-doped TiO₂ nanoparticles at different magnification widths and views fields 5.49mm, 171µm, 5.46mm, 65µm, 5.47mm, 33.3µm, 5.47mm, 16.5µm, 5.49mm, 3.29µm and 5.48mm, 1.67µm respectively(Zhao, Ren, Huang, Chen, & Bian, 2022). In picture E, at the magnification of 1µm, the radius of doped nanoparticles at different points is given at C1 70.38nm, C2 66.15nm, and C3 74.91nm. In the last picture, the magnification of the 500nm radius of doped nanoparticles is like at C1 28.52nm, C2 24.79nm, and C3 28.84nm.

3.2. Elemental Analysis

To find out the elemental composition of prepared samples, EDX is used to analyze the samples. For the elemental analysis or chemical characterization of samples. An analytical technique is called energy-dispersive X-ray spectroscopy, energy dispersive X-ray analysis (EDXA), or energy dispersive X-ray microanalysis (EDXMA) is useful for characterization. The mechanism of this technique is an interaction of X-ray excitation with a sample. A high-energy beam of charged particles such as electrons or protons, or a beam of X-rays, is focused on the samples to stimulate the emission of characteristic X-rays from

samples. An atom within the sample, when at rest, contains ground state electrons in discrete energy levels or electron shells bound to the nucleus(Wang et al., 2022). The incident beam will create the electron-hole pair by exciting an electron from an inner shell. When an electron-hole pair is created, the outer higher-energy shell fills this hole; when an electron of a higher energy level fills this hole, it will release the energy to come down, which will be in the form of an X-ray. This energy released by the electrons and the number of X-rays emitted from a sample will be measured by an instrument called an energy-dispersive spectrometer (Jia et al., 2022).

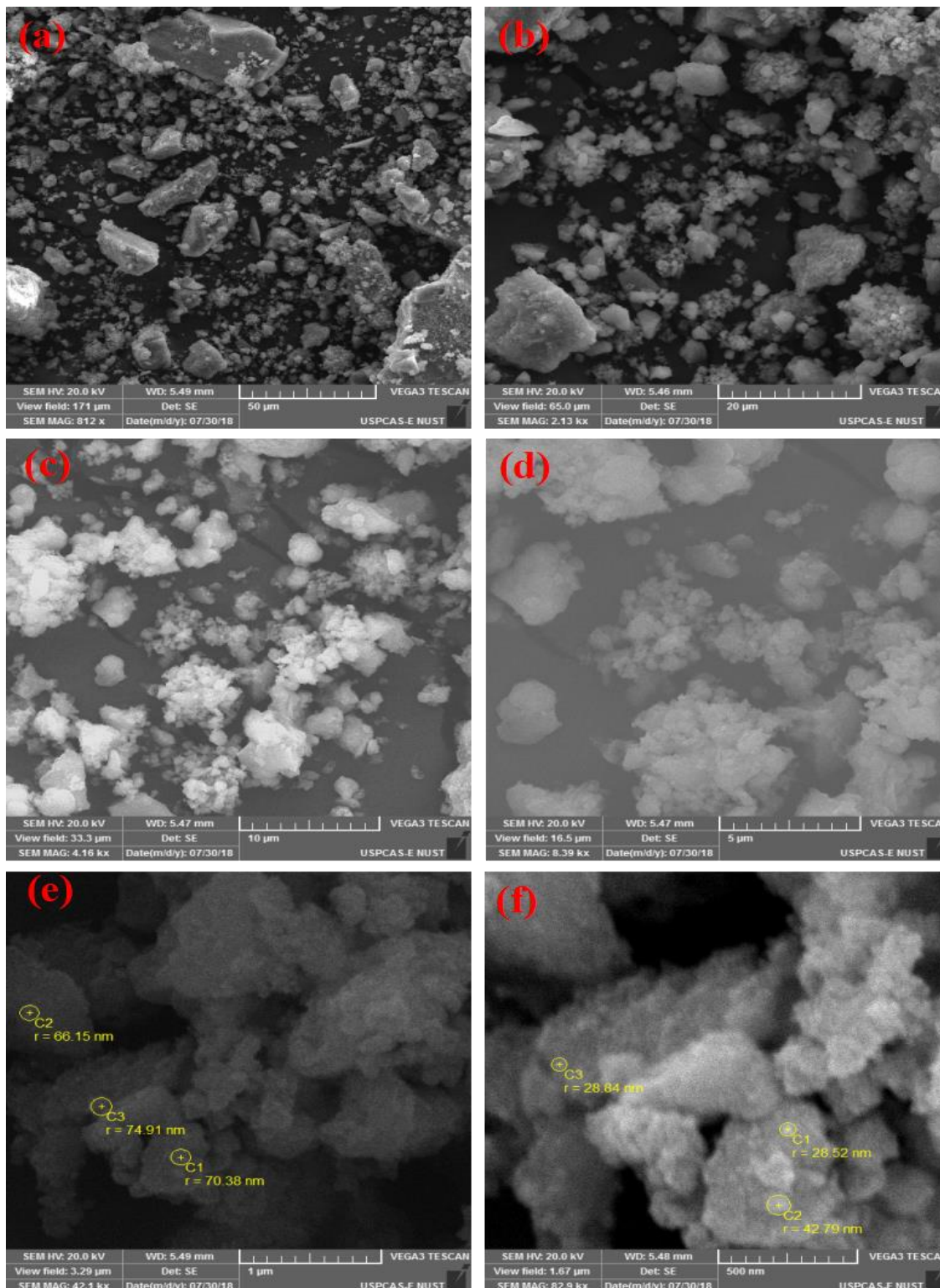


Figure 1: SEM images of Fe-doped TiO₂ Nanoparticles with Different Magnification

EDS allows the elemental composition of the samples to be measured as the energies of the X-rays are characteristics of the difference in energy between the two shells and the atomic structure of the emitting element. After that, the weight percentage of the elements present in the samples can observe. This percentage will be determined by the

technique named Energy Dispersive X-ray Spectrometer. Using this technique, we will know the weight percentage of major and minor elements present in the samples. In the energy dispersive X-ray spectrometer, an accelerating voltage is 20keV(Dharmale, Chaudhury, & Pandey, 2022). The EDX analysis of Fe-doped TiO₂ nanoparticles calcined at 400 °C is shown below. The atomic and the weight percentage of minor and major elements are shown in the tables below.

From the given tables, we can say that elements are present in the samples, such as Ti, O & doped element, which is iron in this case present the samples. doped TiO₂ shows the sample's chemical composition of Ti, O, and Fe in Fe. There are some minor impurity peaks in the pure sample, which were observed in the EDX spectra. It confirms that the prepared samples have some impurities like oxygen and Sulphur. In figure 4.3, there are two different pictures. One is an SEM image at 20µm, and the other shows elemental composition in the sample. From this, it can see. There are various elements like oxygen, Sulphur, and Ti. Ti is the element present in a small amount in the sample, as shown in spectrum 1. There are some other elements present in the sample which show small peaks in spectrum 1. At 0kV and 4kV, peaks show Ti present in a small amount. shows the elemental composition with weight and atomic percentage. From the table, we can say that in the sample, there is Ti which has a 58.11 weight percentage, oxygen has 37.18, and Sulphur has 4.71 %(W. Li et al., 2022).

From this, we can see. There are different elements like oxygen, Sulphur, and Ti. The most amount of Fe is present in spectrum 2. From the figure given below, we can say that there are elements such as Ti, S, O, and Fe in the spectrum. At 6.5keV, there is Fe present in a small amount. It shows that this sample contains the doped element in most amounts. From the given table, we can say that there is a much more weight percentage of Fe than other elements. From the Table, Fe has 77.13, oxygen 12.19, and Ti has 4.31 weight %(Yuzer et al., 2022).

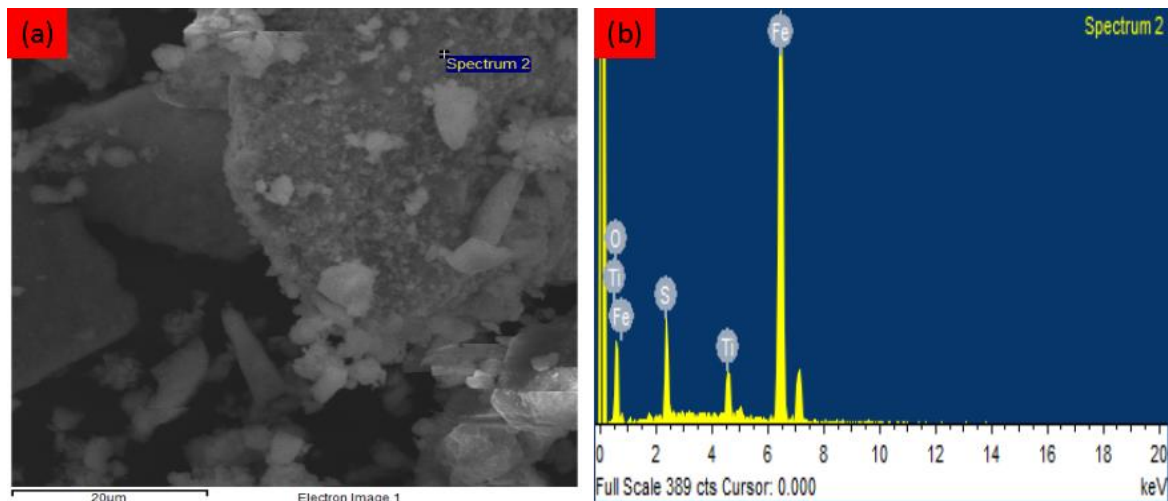


Figure 2: EDX of Fe-Doped TiO₂ Nanoparticles

3.3. Structural Analysis

In this experiment, the physical grinding method is used to get the nanoparticle size of TiO₂ powder. The TiO₂ quantity in powder form is obtained at 8gm. After that, quantity in the mortar and grind, powder form with the help of pestle for 15 minutes to prepare nanoparticles. We turn off fan to avoid impurities like air or dust. After we got nanoparticles size powder, we put this with the help of a spatula into china dishes and then put these china dishes into the furnace just for calcination. After that, we send our sample to Islamabad for XRD analysis. The XRD spectra or technique gives information about the structure, crystallite size, and lattice planes or strain. The broad peaks indicate either particles of a very small crystalline size or semi-crystalline particles. The average crystalline size (the symbol used for crystalline size is D) of titanium dioxide and Fe-doped titanium dioxide nanoparticles was calculated using Debye Scherer's formula. For example, $D = \frac{0.94}{\beta \sin \theta}$, where β is the full width at the half-maximum intensity (FWHM), θ is the diffraction angle, and λ is the wavelength of the X-rays, which is 0.1549 nm or 1.549Å(Yuzer et al., 2022).

The calculated crystallite average radius for titanium dioxide and Fe-doped titanium dioxide was 22 nm and 28 nm, respectively. At some points of the sample where Fe is in very small content (Bhatti, Parikh, & Shah, 2022), the XRD observed no crystalline phase. These results show that the doping of Fe possesses uniform distribution and forms a stable solid solution within titanium dioxide. The diffraction pattern confirmed that the materials prepared in the lab are in the form of small particles because the peaks are broad. The XRD patterns of Fe-doped TiO₂ samples are shown in the figure. From the figures given below, it is clear that up to some peaks of the samples of doped TiO₂ nanoparticles show no structural difference in X-ray spectra. XRD peaks of all the samples where Fe content is very low except where Fe content is most TiO₂ corresponding to the anatase phase. The intensity of the main anatase peak (101) at $2\theta = 25.27$ decreased considerably compared to the pure sample. The peaks at 2θ , i.e., 25.24, 39.11, 47.93, and 54.34 degrees related to lattice planes (101), (200), (111), (210), and (002), which are compatible with rutile phase (JCPDS 21-1276) (Abraham & Devi, 2022). From this, we can see clearly that up to the small content of Fe, the TiO₂ powders exhibit an anatase phase, and a clear phase transformation from the anatase to rutile occurs as doping of Fe increases. These graphs were made in the software named origin 8 pros.

In the graphs of doped TiO₂ nanoparticles, we took on X-axis 2 theta in degree. On Y-axis, we took intensity in a.u. On X-axis, we start from 20 degrees and end at 60 degrees by a difference of 10 degrees. From the first graph below, the first peak is shown (101), which is the main peak. And in the second graph, we also took on X-axis 2 theta in degree, and on Y-axis, we took intensity in a.u. On X-axis, we start from 20 degrees and end at 60 degrees by a difference of 10 degrees. This first peak is also (101), which is the main peak but shows a difference compared to the peak of pure because it is a wide and small peak. The figure shows the XRD spectra of Fe doped TiO₂ nanoparticles, respectively.

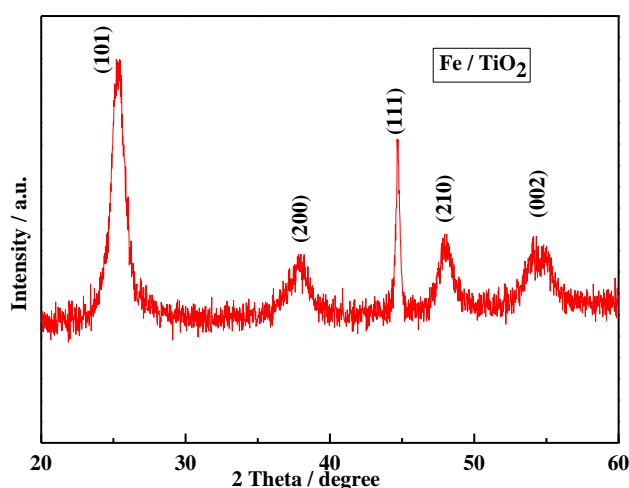


Figure 3: XRD Spectra of Fe-doped TiO₂ Nanoparticles

3.4. UV/Vis Spectra Analysis

To observe the prepared samples technique is used named UV-visible spectroscopy. This technique measured the scattering and absorption of light. The light passes through a sample as the sample is in the form of nanoparticles. And these particles have unique optical properties like size, concentration, shape, agglomeration state, and reflective index. Therefore, UV-Visible is a valuable tool for characterizing, identifying, and studying nanoparticles. For studying UV-Visible spectral, the prepared sample of doped TiO₂ nanoparticles Lambda 35 model UV-Visible spectrometer ranged from 300 to 900nm. Absorption spectroscopy was used to find and explore prepared nanoparticles' optical properties, a powerful non-destructive technique. The UV-Visible spectral studies of the Fe-doped TiO₂ nanoparticle are shown below. The doped TiO₂ nanoparticles were calcined at 500°C (Zhang, Zhang, Zhong, & Ding, 2022). The visible light strongly exhibits photon absorption and produces high photocatalytic activity. These results concluded that the Fe-doped TiO₂ nanoparticles exhibit higher absorption than the pure sample. The absorption spectrum of Fe-doped TiO₂ shows broader absorption in the entire visible region. It is a good condition for solar cell applications. The energy gaps of doped TiO₂ show high

absorption occurs mostly invisible region for doped TiO₂ nanoparticles. Fe doped TiO₂ samples' absorption spectra exhibit strong and broad absorption. It is an excellent understanding of the band gap of the anatase phase. The lowest bandgap value of doped TiO₂ nanoparticles exhibits the rutile phase, and the size of the particle becomes bigger (Sakfali, Ben Chaabene, Akkari, & Zina, 2022). We prepared the Fe-doped TiO₂ nanoparticles sample in the lab and then observed their UV-Visible spectrum. These are the UV-Visible spectrum of prepared nanoparticles, which are given below in the form of a graph.

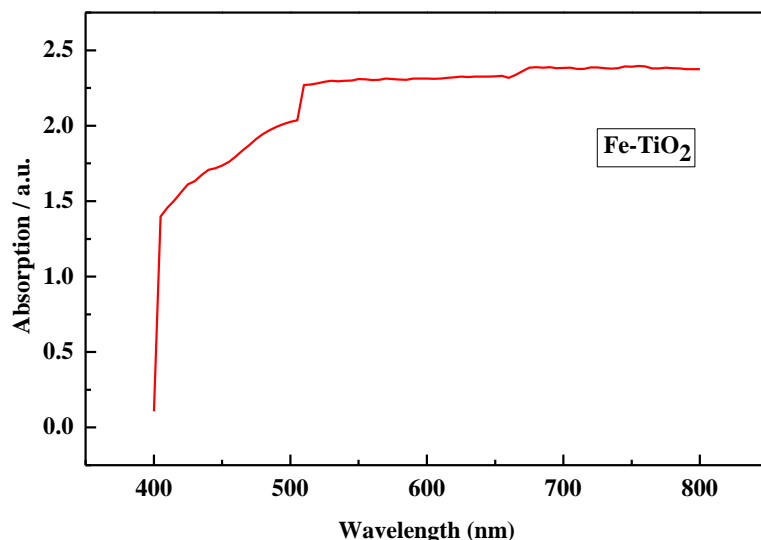


Figure 4: UV/Vis Spectrum of Fe-doped TiO₂ Nanoparticles

Acknowledgments

This work was supported by the Higher Education Commission (HEC) of Pakistan under Grant # 9371/Punjab/ NRPU/R&D/HEC/2017.

References

- Abraham, C., & Devi, L. G. (2022). Incorporation of Fe³⁺ ions into the W⁶⁺ and N³⁻-doped TiO₂: Exploration of crucial role of Fe³⁺ dopant ion and correlation of adsorption characteristics with reaction dynamics. *Surface Science*, *717*, 121986.
- Ali, T., Tripathi, P., Azam, A., Raza, W., Ahmed, A. S., Ahmed, A., & Muneer, M. (2017). Photocatalytic performance of Fe-doped TiO₂ nanoparticles under visible-light irradiation. *Materials Research Express*, *4*(1), 015022.
- Baruah, M., Ezung, S. L., Supong, A., Bhomick, P. C., Kumar, S., & Sinha, D. (2021). Synthesis, characterization of novel Fe-doped TiO₂ activated carbon nanocomposite towards photocatalytic degradation of Congo red, E. coli, and S. aureus. *Korean Journal of Chemical Engineering*, *38*(6), 1277-1290.
- Begna, W. B., Gurmesa, G. S., Zhang, Q., & Geffe, C. A. (2022). A DFT+ U study of site dependent Fe-doped TiO₂ diluted magnetic semiconductor material: Room-temperature ferromagnetism and improved semiconducting properties. *AIP Advances*, *12*(2), 025002.
- Bhatti, D. T., Parikh, S. P., & Shah, M. (2022). A statistical modeling-optimization approach for photocatalytic degradation of difluoro triazole acetophenone using Ag-Fe co-doped TiO₂: response surface methodology. *Environmental Science and Pollution Research*, 1-16.
- Dharmale, N., Chaudhury, S., & Pandey, C. K. (2022). Theoretical investigation on undoped and doped TiO₂ for solar cell application. *Physica Scripta*, *97*(5), 055806.
- Dholam, R., Patel, N., Adami, M., & Miotello, A. (2009). Hydrogen production by photocatalytic water-splitting using Cr-or Fe-doped TiO₂ composite thin films photocatalyst. *International Journal of Hydrogen Energy*, *34*(13), 5337-5346.

- Einert, M., Hartmann, P., Smarsly, B., & Brezesinski, T. (2021). Quasi-homogenous photocatalysis of quantum-sized Fe-doped TiO₂ in optically transparent aqueous dispersions. *Scientific reports*, 11(1), 1-10.
- Jia, M., Liu, Q., Xiong, W., Yang, Z., Zhang, C., Wang, D., . . . Cao, J. (2022). Ti³⁺ self-doped TiO₂ nanotubes photoelectrode decorated with Ar-Fe₂O₃ derived from MIL-100 (Fe): Enhanced photo-electrocatalytic performance for antibiotic degradation. *Applied Catalysis B: Environmental*, 310, 121344.
- Kanjana, N., Maiaugree, W., Poolcharuansin, P., & Laokul, P. (2021). Synthesis and characterization of Fe-doped TiO₂ hollow spheres for dye-sensitized solar cell applications. *Materials Science and Engineering: B*, 271, 115311.
- Kim, D. H., Hong, H. S., Kim, S. J., Song, J. S., & Lee, K. S. (2004). Photocatalytic behaviors and structural characterization of nanocrystalline Fe-doped TiO₂ synthesized by mechanical alloying. *Journal of Alloys and Compounds*, 375(1-2), 259-264.
- Larumbe, S., Monge, M., & Gómez-Polo, C. (2015). Comparative study of (N, Fe) doped TiO₂ photocatalysts. *Applied Surface Science*, 327, 490-497.
- Li, W., Zhou, L., Xie, L., Kang, K., Xu, J., & Chai, X. (2022). N-Fe-Gd co-doped TiO₂/g-C₃N₄ nanosheet hybrid composites with superior photocatalytic dye degradation. *Advanced Composites and Hybrid Materials*, 5(1), 481-490.
- Li, Z., Shen, W., He, W., & Zu, X. (2008). Effect of Fe-doped TiO₂ nanoparticle derived from modified hydrothermal process on the photocatalytic degradation performance on methylene blue. *Journal of hazardous materials*, 155(3), 590-594.
- Na, K.-H., Kim, B.-S., Yoon, H.-S., Song, T.-H., Kim, S.-W., Cho, C.-H., & Choi, W.-Y. (2021). Fabrication and photocatalytic properties of electrospun Fe-doped TiO₂ nanofibers using polyvinyl pyrrolidone precursors. *Polymers*, 13(16), 2634.
- Nasralla, N., Yeganeh, M., Astuti, Y., Piticharoenphun, S., Shahtahmasebi, N., Kompany, A., . . . Siller, L. (2013). Structural and spectroscopic study of Fe-doped TiO₂ nanoparticles prepared by sol-gel method. *Scientia Iranica*, 20(3), 1018-1022.
- Sakfali, J., Ben Chaabene, S., Akkari, R., & Zina, M. S. (2022). One-Pot Sol-Gel Synthesis of Doped TiO₂ Nanostructures for Photocatalytic Dye Decoloration. *Russian Journal of Inorganic Chemistry*, 1-14.
- Song, G., Gao, R., Zhao, Z., Zhang, Y., Tan, H., Li, H., . . . Feng, M. (2022). High-spin state Fe (III) doped TiO₂ for electrocatalytic nitrogen fixation induced by surface F modification. *Applied Catalysis B: Environmental*, 301, 120809.
- Sood, S., Umar, A., Mehta, S. K., & Kansal, S. K. (2015). Highly effective Fe-doped TiO₂ nanoparticles photocatalysts for visible-light driven photocatalytic degradation of toxic organic compounds. *Journal of colloid and interface science*, 450, 213-223.
- Sukhadeve, G., Janbandhu, S., Kumar, R., Lataye, D., Ramteke, D., & Gedam, R. (2022). Visible light assisted photocatalytic degradation of Indigo Carmine dye and NO₂ removal by Fe doped TiO₂ nanoparticles. *Ceramics International*.
- Valero-Romero, M., Santaclara, J., Oar-Arteta, L., Van Koppen, L., Osadchii, D., Gascon, J., & Kapteijn, F. (2019). Photocatalytic properties of TiO₂ and Fe-doped TiO₂ prepared by metal organic framework-mediated synthesis. *Chemical Engineering Journal*, 360, 75-88.
- Wang, J., Wang, Z., Zhao, D., Liang, Y., Wang, H., Wang, N., . . . Ding, W. (2022). Preparation, structural and photocatalytic activity of Sn/Fe co-doped TiO₂ nanoparticles by sol-gel method. *Ceramics International*, 48(6), 8297-8305.
- Xia, Z., Xing, S., Wang, H., Zhao, D., Wu, S., Jiang, W., . . . Ding, W. (2022). Weak-visible-light-driven Fe doped TiO₂ photocatalyst prepared by coprecipitation method and degradation of methyl orange. *Optical Materials*, 129, 112522.
- Yu, J., Yu, H., Ao, C., Lee, S., Jimmy, C. Y., & Ho, W. (2006). Preparation, characterization and photocatalytic activity of in situ Fe-doped TiO₂ thin films. *Thin Solid Films*, 496(2), 273-280.
- Yuzer, B., Aydın, M. I., Con, A. H., Inan, H., Can, S., Selcuk, H., & Kadmi, Y. (2022). Photocatalytic, self-cleaning and antibacterial properties of Cu (II) doped TiO₂. *Journal of Environmental Management*, 302, 114023.
- Zhang, H., Zhang, Y., Zhong, Y., & Ding, J. (2022). Novel strategies for 2, 8-dichlorodibenzo-p-dioxin degradation using ternary Au-modified iron doped TiO₂ catalysts under UV-vis light illumination. *Chemosphere*, 291, 132826.
- Zhao, Q., Ren, Y., Huang, L., Chen, Y., & Bian, Z. (2022). In situ Fe (III)-doped TiO₂ mesocrystals catalyzed visible light photo-Fenton system. *Catalysis Today*.

Zheng, X., Li, Y., You, W., Lei, G., Cao, Y., Zhang, Y., & Jiang, L. (2022). Construction of Fe-doped TiO₂-x ultrathin nanosheets with rich oxygen vacancies for highly efficient oxidation of H₂S. *Chemical Engineering Journal*, 430, 132917.